

**PREPARATION AND
CHARACTERIZATION OF GRAPHENE
OXIDE – ZINC OXIDE NANOCOMPOSITE
IN DEGRADATION OF PHENANTHRENE
FROM AQUEOUS SOLUTIONS**

HUSN ARA CHAUHAN

UNIVERSITI SAINS MALAYSIA

2022

**PREPARATION AND
CHARACTERIZATION OF GRAPHENE
OXIDE - ZINC OXIDE NANOCOMPOSITE
IN DEGRADATION OF PHENANTHRENE
FROM AQUEOUS SOLUTIONS**

by

HUSN ARA CHAUHAN

**Thesis submitted in fulfilment of the requirements
for the degree of
Master of Science**

September 2022

ACKNOWLEDGEMENT

I offer Allah praise and appreciation for His favours and kindness in enabling me to begin and complete the master' degree programme. My sincere gratitude and admiration go to my supervisor, Assoc. Prof. Dr. Mohd. Rafatullah, co-supervisor, Dr. Khozema Ahmed Ali, laboratory staff, and colleagues have contributed to the fruitfulness and satisfaction of my academic career at Universiti Sains Malaysia (USM). My supervisor gave me enough advice and assistance, which aided in the project's success. I appreciate my colleagues from the School of Industrial Technology for their support and guidance at different points in the research process. My accomplishment would have been unthinkable without the financial support, encouragement, and love of my parents, the late Abdulli Khan and Fatima Begum. They motivated me to achieve this level of success and pursue my passion. Additionally, I cannot quantify my sister's encouragement and spiritual support, Dr Razia Chauhan, and my brothers, Javed Ali Khan, Asif Ali Khan, and Arif Ali Khan. I met my friends who turned into a family during my sojourn in USM, and I want to say a very big thank you to Aseel Yaghi, Kaif Mahmood, Sarika Verma, Intekhab Hussain, Mohammad Faisal Umar, and Hanadi Ahmad. I appreciate your encouragement during trying times and the memories we made together.

Finally, I would like to thank the “Ministry of Higher Education Malaysia for the Fundamental Research Grant Scheme with Project Code: FRGS/1/2019/STG07/USM/02/12”, which enabled me to conduct a successful research project.

TABLE OF CONTENTS

ACKNOWLEDGEMENT	ii
TABLE OF CONTENTS	iii
LIST OF TABLES	vi
LIST OF FIGURES	vii
LIST OF SYMBOLS AND ABBREVIATIONS	ix
ABSTRAK	xv
ABSTRACT	xvii
CHAPTER 1 INTRODUCTION	1
1.1 Research background	1
1.1.1 Problem statement	7
1.1.2 Research questions	9
1.1.3 Objectives.....	9
1.1.4 Scope and approach.....	10
1.1.5 Significance	12
1.1.6 Thesis organization	12
CHAPTER 2 LITERATURE REVIEW	14
2.1 Photocatalytic degradation of phenanthrene	14
2.2 Types of photocatalysts for the degradation of phenanthrene.....	18
2.2.1 Titanium dioxide-based photocatalysts	18
2.2.2 Iron-based photocatalysts	29
2.2.3 Silver-based photocatalysts	35
2.2.4 Carbon-based photocatalysts	40
2.2.5 Zinc-based photocatalysts	43
2.3 Mechanism and degradation pathways of phenanthrene.....	46
2.4 Summary	57

CHAPTER 3	METHODOLOGY	59
3.1	Introduction	59
3.2	Materials and chemicals	61
3.3	Preparation of nanocomposites	62
3.3.1	Preparation of rice husk derived graphite powder	62
3.3.2	Synthesis of graphene oxide (GO)	63
3.3.3	Synthesis of graphene oxide-zinc oxide (GO/ZnO) nanocomposite.....	64
3.4	Characterization of nanocomposites	65
3.4.1	X-ray diffractometry analysis.....	66
3.4.2	Scanning electron microscope (SEM) and Energy dispersive X-ray analysis (EDX).....	66
3.4.3	Ultraviolet-visible diffuse reflectance spectroscopy analysis	66
3.4.4	Brunauer-Emmett-Teller analysis	67
3.4.5	Transmission electron microscope (TEM) analysis.....	67
3.4.6	Fourier transform infrared spectroscopy analysis	68
3.4.7	Raman analysis.....	68
3.5	Photocatalytic Action	68
CHAPTER 4	RESULTS AND DISCUSSION	74
4.1	Introduction	74
4.2	Characterization	74
4.2.1	Fourier transform infrared analysis	74
4.2.2	UV-Visible Diffuse Reflectance Spectroscopy Analysis.....	76
4.2.3	X-Ray Diffraction Analysis	78
4.2.4	Raman Analysis.....	80
4.2.5	Scanning Electron Microscopy and Energy Dispersive X-Ray Analysis.....	81
4.2.6	Transmission Electron Microscopy (TEM)	83

4.2.7	Brunauer-Emmett-Teller (BET) Analysis.....	84
4.3	Assessment of Photocatalytic Activity.....	85
4.3.1	Effect of phenanthrene concentration	88
4.3.2	Effect of GO/ZnO Dosage.....	89
4.3.3	Effect of pH.....	91
4.3.4	Reaction Kinetics	93
4.4	Photocatalytic Degradation Pathways of Phenanthrene using GO/ZnO Nanocomposite	95
4.5	Comparison with Other Catalysts	96
4.6	Reusability of the Photocatalyst	100
CHAPTER 5 CONCLUSION AND FUTURE RECOMMENDATIONS....		101
5.1	Conclusions	101
5.2	Recommendations for Future Research	103
REFERENCES.....		105
LIST OF PUBLICATIONS		

LIST OF TABLES

	Page
Table 2.1	List of titanium dioxide-based photocatalysts and its various parameters for the degradation of phenanthrene.24
Table 2.2	List of iron-based photocatalysts and its various parameters for the degradation of phenanthrene.32
Table 2.3	List of silver-based photocatalysts and its various parameters for the degradation of phenanthrene.37
Table 2.4	List of carbon-based photocatalysts and its various parameters for the degradation of phenanthrene.41
Table 2.5	List of zinc-based photocatalysts and its various parameters for the degradation of phenanthrene.45
Table 2.6	Degradation products of phenanthrene by different catalysts.50
Table 3.1	List of materials and chemicals.61
Table 4.1	Rate constants, half-life, correlation coefficient, and degradation efficiency values of phenanthrene with nanocatalysts under optimal circumstances.94
Table 4.2	Comparison data of phenanthrene photodegradation reported by other studies.96

LIST OF FIGURES

	Page
Figure 1.1	Schematic representation of environmental remediation of phenanthrene by photocatalysis.....6
Figure 2.1	The implemented degradation of phenanthrene by photocatalysis intervened by GO/ZnO nanocomposite..... 17
Figure 2.2	The implemented degradation of phenanthrene by photocatalysis intervened by photogenerated OH● radical and hole.....47
Figure 3.1	Flowchart of experiment for the degradation of phenanthrene by photocatalysis under UV-Visible light.60
Figure 3.2	(a) Rice husk ash (RHA), (b) Vacuum filtration of graphite, and (c) Dried Graphite powder.63
Figure 3.3	The synthesized product of GO.....64
Figure 3.4	Dried product of GO/ZnO nanocomposite.65
Figure 3.5	Outside and inside photocatalytic reactor design.69
Figure 4.1	FTIR analysis of graphite, GO, and GO/ZnO nanocomposite.76
Figure 4.2	UV-Visible DRS spectroscopy analysis of GO and GO/ZnO nanocomposite.77
Figure 4.3	Tauc plot to determine the optical band gap of GO/ZnO nanocomposite.78
Figure 4.4	XRD analysis of graphite, GO, and GO/ZnO nanocomposite.79
Figure 4.5	Raman spectra analysis of graphite, GO, and GO/ZnO nanocomposite.81
Figure 4.6	SEM images of (a) and (b) GO; (c) and (d) GO/ZnO nanocomposite.82
Figure 4.7	EDX micrograph; (a) and (b) GO; (c) and (d) GO/ZnO nanocomposite at different magnifications.....83

Figure 4.8	TEM images of (a) GO, and (b) GO/ZnO nanocomposite.....	84
Figure 4.9	(a) Type IV N ₂ adsorption-desorption isotherm for the BET surface area analysis of GO/ZnO nanocomposite, and (b) Pore size distribution of GO/ZnO nanocomposite.....	85
Figure 4.10	Percentage of phenanthrene degradation by GO/ZnO nanocomposite, followed by photolysis (no photocatalyst), GO/ZnO without stirring, GO/ZnO in dark with stirring, commercial ZnO, and GO/ZnO.....	86
Figure 4.11	Effect of UV-Visible irradiation on phenanthrene (25 ppm) degradation by GO/ZnO photocatalyst (2 g/L) in aqueous solution. .	87
Figure 4.12	Schematic illustration depicting degradation method of phenanthrene by utilizing GO/ZnO photocatalyst in the presence of UV-Visible light.....	88
Figure 4.13	Effect of phenanthrene concentrations.	89
Figure 4.14	Effect of GO/ZnO nanocomposite dosages.	91
Figure 4.15	Effect of initial pH on the degradation of phenanthrene.	93
Figure 4.16	Linearized first-order model fittings of the kinetic data for the degradation of phenanthrene (25 ppm).....	94
Figure 4.17	Total ion chromatograms of degraded phenanthrene (a) in 6 hours, (b) in 9 hours, and (c) proposed degradation pathway for the degradation of phenanthrene over GO/ZnO nanocomposite (Concentration: 25 ppm; pH: 6.80, photocatalyst dose: 2g/L; UV-Visible light).	96
Figure 4.18	Reusability analysis of GO/ZnO nanocomposite for phenanthrene degradation.	100

LIST OF SYMBOLS AND ABBREVIATIONS

%	Percentage
e^-/h^+	Electron-hole pair
e^-h^+	Electron-hole pair
•	Free radical
λ	wavelength
meV	millielectronvolt
eV	Electron volt
$^{\circ}\text{C}$	Degree Celsius
nm	Nanometer
mg	milligram
hr	Hour
mg/L	milligram per litre
W/m^2	Watt per square meter
mW/cm^2	milliWatt per square centimetre
PAHs	Polycyclic Aromatic Hydrocarbons
USEPA	US Environmental Protection Agency
ZnO	Zinc oxide
TiO ₂	Titanium dioxide
GO	Graphene oxide
rGO	Reduced graphene oxide
GO-CuO	Graphene oxide-cupric oxide
GO/ZnO	Graphene oxide-zinc oxide
UV	Ultraviolet
NiO	Nickel oxide
In ₂ O ₃	Indium oxide

$\alpha\text{-Fe}_2\text{O}_3$	Hematite
CB	Conduction band
VB	Valence band
$\cdot\text{OH}$	Hydroxide radical
$\cdot\text{O}_2^-$	Superoxide radical
H_2O	Water
CO_2	Carbon dioxide
$\text{TiO}_2@\text{ZnHCF}$	Titanium dioxide-based zinc hexacyanoferrate
Co-TNTs-600	Cobalt deposited titanate nanotubes
Pt/ $\text{TiO}_2\text{-SiO}_2$	Platinum deposited titanium dioxide-silicon dioxide
$\text{WO}_3@$ anatase- SiO_2	Tungsten trioxide@anatase-silicon dioxide
GO- $\text{TiO}_2\text{-Sr}(\text{OH})_2/\text{SrCO}_3$ FeCo-BDC	Graphite oxide- titanium dioxide-strontium hydroxide- strontium carbonate 1,4-benzenedicarboxylic acid metalloligand unit linked by Fe(II) and Co(II) cations
MIL	Materials Institute Lavoisier
-OH	Hydroxyl group
NH_2	Amino group
-COOH	Carboxyl group
NO_2	Nitrogen dioxide
-H	Hydrogen
Fe^{3+}	Ferric ion
CA	Citric Acid
FeHCF	Iron hexacyanoferrate
Ca- Ag_3PO_4	Calcium based silver phosphate
$\text{Mn}_3\text{O}_4/\text{MnO}_2\text{-cubic } \text{Ag}_3\text{PO}_4$ GO/ Ag_3PO_4	Trimanganese tetraoxide/manganese dioxide-cubic silver phosphate Graphene oxide enwrapped silver phosphate
$\text{Ag}_3\text{PO}_4/\text{GO}$	Graphene oxide enwrapped silver phosphate
SSNT@GQD	Stainless-steel nanotubes with graphene quantum dots

NiO-ZnO	Nickel oxide-zinc oxide
ZnS	Zinc sulfide
Ag ₂ S	Silver (I) sulfide
O ₂	Oxygen
Zn ²⁺	Zinc ion
TiO ₂ /TiNTs	Titanate nanotubes supported titanium dioxide
Na	Sodium
mg/g	Milligram per gram
K _{obs}	Rate constant
PMR	Photocatalytic membrane reactor
h ⁻¹	Per hour
BaP	Benzo[a]pyrene
DahA	Dibenzo[a]anthracene
H ₂ O ₂	Hydrogen peroxide
ph	phenanthrene
DFT	Density Functional Theory
DMC	Dimethyl carbonate
MPTES/TiO ₂	1,4-benzenedicarboxylic acid doped with titanium dioxide
N ₂	Nitrogen
GC-MS	Gas chromatography-mass spectrometry
g/L	Gram per litre
µg/L	Microgram per litre
temp.	Temperature
conc.	Concentration
µg/mL	Microgram per millilitre
NA	Not available
M	Molar

min	Minute
mol/g	Moles per gram
wt. %	Weight %
mM	Millimoles
PS	Persulfate
HPLC	High Performance Liquid Chromatography
mm	Millimeter
μm	Micrometer
id.	Internal diameter
Xe	Xenon
DAD	Diode Array Detector
mW/m ²	milliWatt per square meter
W	Watt
XPS	X-ray Photoelectron Microscopy
SEM	Scanning Electron Microscopy
XRD	X-ray Diffraction
FT-IR	Fourier Transform Infrared
UV-Vis DRS	UV-Visible Diffuse Reflectance Spectroscopy
TEM	Transmission Electron Microscopy
EDX	Energy Dispersive X-ray
BET	Brunauer-Emmett-Teller
ICP-MS	Inductively Coupled Plasma Mass Spectrometry
PMS	Peroxymonosulfate
m ² /g	Square meter per gram
mV	millivolt
VPCB	Visible-light induced Photocatalysis and Biodegradation
VPC	Visible-light induced Photocatalysis

g-C ₃ N ₄	Graphitic carbon nitride
min ⁻¹	Per minute
BMO	Bimetallic oxides
ROS	Reactive oxygen species
m/z	Mass to charge ratio
Pt-TaON	Pt-tantalum oxynitride
KZnHCF	Potassium zinc hexacyanoferrate
SO ₄ ^{•-}	Sulphate ion
h ⁺	hole
RHA	Rice husk ash
KOH	Potassium hydroxide
rpm	Rounds per minute
NaNO ₃	Sodium nitrate
HCl	Hydrochloric acid
KMnO ₄	Potassium permanganate
PTFE	Polytetrafluoroethylene
H ₂ SO ₄	Sulfuric acid
ppm	Parts per million
mL/min	Millilitre per minute
C _o	Initial concentration
C _t	Concentration at a time, t
t	Time
kV	kilovolt
mA	milliampere
cm ³ /g STP	Cubic centimeter per gram at Standard Temperature and Pressure
P/P _o	Relative pressure
KBr	Potassium bromide

C=C	sp ² carbon
C-OH	Tertiary alcohol
C-O	Epoxy and alkoxy group
C=O	Carbonyl group
K	kelvin
Eqs.	Equations
e ⁻	Electron
R ²	correlation coefficient
t _{1/2}	half-life
η	Degradation efficiency
K	Rate constant
WHO	World Health Organization

**PENYEDIAAN DAN PENCIRIAN GRAPHENE OKSIDA – ZINK
OKSIDA KOMPOSIT NANO DALAM DEGRADASI PHENANTHRENE
DARIPADA LARUTAN AKUEUS**

ABSTRAK

Kebimbangan alam sekitar telah timbul kerana sifat berterusan dan kekarsinogenan hidrokarbon aromatik polisiklik (PAH). Kanser kulit, paru-paru, pankreas, esofagus, pundi kencing, kolon dan payudara wanita hanyalah sebahagian daripada organ yang dikaitkan dengan pendedahan PAH jangka panjang. Telah dicadangkan bahawa terdedah kepada PAH juga meningkatkan kemungkinan mendapat kanser paru-paru. Oleh itu, penggunaan nanokomposit dengan kecekapan tinggi adalah perlu. Kajian ini menggunakan pendekatan doping untuk berjaya membina fotomangkin nanokomposit berasaskan graphene oksida (GO) dan zink oksida (ZnO). Nanokomposit telah disiasat oleh spektroskopi inframerah transformasi Fourier (FTIR), spektroskopi pemantulan resap UV-Visible (UV-Vis DRS), pembelauan sinar-X (XRD), spektroskopi Raman, mikroskopi elektron pengimbasan (SEM) dengan sinar-X penyebaran tenaga (EDX), mikroskop elektron penghantaran (TEM), Brunauer-Emmett-Teller (BET). Aktiviti fotokatalitik nanokomposit yang disintesis telah diuji dalam kemerosotan fenantrina sebagai pelopor bahan cemar dalam air. Pada pH 6.8, nanokomposit GO/ZnO menunjukkan keupayaan yang sangat baik untuk merendahkan 25 ppm fenantrina (86.06%) dalam 120 minit di bawah pendedahan cahaya UV-Visible diikuti oleh ZnO komersial (62.84%), GO/ZnO dalam gelap dengan kacau (47.40. %), GO/ZnO tanpa kacau (40.28%), dan fotolisis (tiada fotomangkin) (15.56%). Ini disebabkan oleh kawasan permukaan terbesar (15.39845 m²/g), yang dipertingkatkan oleh doping GO dalam

ZnO komersial. Fotodegradasi Phenanthrene oleh nanokomposit GO/ZnO mengikuti kinetik tertib pertama dengan pemalar kadar 0.0375 min⁻¹. Hasil sampingan yang lebih kecil seperti (Z)-3-hidroksi asid akrilik (1b; m/z = 88) dan (Z)-4-oxobut-2-enoic acid (1c; m/z = 100) yang dikenal pasti dalam GC-MS, jelas menunjukkan e-keterujaan daripada pemangkin foto yang digabungkan diikuti oleh pengoksidaan fenantrina berasaskan •OH (spesies aktif). Selain itu, nanokomposit GO/ZnO mempamerkan jurang jalur 3.16 eV. Disebabkan lebih banyak bahan pencemar yang terserap ke permukaan fotomangkin dan pengurangan dalam jurang jalur, kadar penggabungan semula berkurangan, dan penyerapan cahaya beralih ke kawasan yang boleh dilihat, membolehkan nanokomposit GO/ZnO menggunakan cahaya matahari dengan lebih cekap dan mempercepatkan degradasi fenantrina. Komposit yang disintesis adalah stabil dan boleh dihasilkan semula, kerana kecekapan degradasinya berkurangan sebanyak 1% sahaja selepas empat kitaran yang berjaya. Akibatnya, nanokomposit GO/ZnO boleh menjadi fotomangkin serba boleh untuk fotodegradasi fenantrina dalam rawatan air sisa.

**PREPARATION AND CHARACTERIZATION OF GRAPHENE
OXIDE - ZINC OXIDE NANOCOMPOSITE IN DEGRADATION
OF PHENANTHRENE FROM AQUEOUS SOLUTIONS**

ABSTRACT

Environmental concerns have arisen due to the persistent nature and carcinogenicity of polycyclic aromatic hydrocarbons (PAHs). Skin, lung, pancreatic, oesophageal, bladder, colon, and female breast cancer are only some of the organs that have been linked to long-term PAH exposure. It has been suggested that being exposed to PAH also raises the odds of developing lung cancer. Thus, the use of nanocomposites with high-efficiency properties is necessary. This study used the doping approach to successfully construct a nanocomposite photocatalyst based on graphene oxide (GO) and zinc oxide (ZnO). The nanocomposites were investigated by Fourier transform infrared (FTIR) spectroscopy, UV-Visible diffuse reflectance spectroscopy (UV-Vis DRS), X-ray diffraction (XRD), Raman spectroscopy, scanning electron microscopy (SEM) with energy dispersive X-ray (EDX), transmission electron microscopy (TEM), Brunauer-Emmett-Teller (BET). The photocatalytic activity of synthesized nanocomposites was tested in phenanthrene deterioration as a precursor of contaminants in water. At 6.8 pH, the GO/ZnO nanocomposite showed excellent ability to degrade 25 ppm of phenanthrene (86.06%) in 120 minutes under UV-Visible light exposure followed by commercial ZnO (62.84%), GO/ZnO in the dark with stirring (47.40%), GO/ZnO without stirring (40.28%), and photolysis (no photocatalyst) (15.56%). This is due to the largest surface area (15.39845 m²/g), which was enhanced by the doping of GO in commercial ZnO. Phenanthrene photodegradation by GO/ZnO nanocomposite

followed first-order kinetics with a rate constant of 0.0375 min^{-1} . The smaller byproducts like (Z)-3-hydroxy acrylic acid (1b; $m/z = 88$) and (Z)-4-oxobut-2-enoic acid (1c; $m/z = 100$) identified in GC-MS, clearly demonstrated e^- excitement from incorporated photocatalyst followed by $\bullet\text{OH}$ (active species) based oxidation of phenanthrene. Moreover, the GO/ZnO nanocomposite exhibits a bandgap of 3.16 eV. Due to more pollutants adsorbing onto the photocatalyst surface and the reduction in bandgap, the recombination rate decreased, and the light absorption shifted into the visible region, allowing the GO/ZnO nanocomposite to utilise sunlight more efficiently and accelerate the degradation of phenanthrene. The synthesised composite is stable and reproducible, as its degradation efficiency decreased by only 1% after four successful cycles. Consequently, the GO/ZnO nanocomposite could be a versatile photocatalyst for the photodegradation of phenanthrene in wastewater treatment.

CHAPTER 1

INTRODUCTION

1.1 Research background

Polycyclic aromatic hydrocarbons (PAHs) are long-lasting compounds that can accrue in animals and plants as they move up the food chain. As a result, PAHs were identified in a wide range of marine habitats, including polluted water treatment facilities, underground water, and saltwater (Wei et al., 2022; Zhou et al., 2019). The International Agency for Research on Cancer has identified PAHs as likely carcinogens, posing a risk to human health and ecosystems. Furthermore, the US Environmental Protection Agency (USEPA) has categorized some PAHs as primary regulated pollutants (Lamichhane et al., 2016). The name phenanthrene is created from different terms: “phenyl” and “anthracene”, previously known as benzene. As a recognized contaminant, it has been studied extensively in many matrices. Phenanthrene was the most prevalent PAH in tap water, accounting for around one-third of the sixteen USEPA priority PAHs, according to one reported article (Ying Zhang et al., 2019). A considerable amount of phenanthrene was released into the environment by manufacturing coke, liquefaction of fossil fuels, and volcanic eruptions (Han et al., 2019). The petrochemical industry located at Khapri in outskirts of Nagpur, India has been dumping petrochemical waste effluent containing a mixture of PAHs such as phenanthrene at this site via underground waste effluent lines for the past three decades (Janbandhu & Fulekar, 2011). Phenanthrene's ozonation products cause hepatic toxicity than phenanthrene itself, with the probable impact of nephrotoxicity (Kasumba & Holmén, 2018). As a result of this compound's widespread distribution and destructive potential, it is critical to track it down and

remove it from the ecosystem. Given the threats or concerns posed by specific PAHs and associated metabolites, hourly needs for sophisticated water treatment systems (that are effective, cheap, and/or convenient to control) have evolved. The discovery of effective methods for removing phenanthrene from aqueous solutions has garnered considerable interest during the last few decades. Numerous approaches, including chemical oxidation, microbial degradation, phytoremediation, adsorption, and chemical precipitation have been used (Mojiri et al., 2019). However, the adsorbent used in the adsorption process is crucial for maximizing the removal method's efficiency (Lingamdinne et al., 2018). Multi walled carbon nanotubes have a greater capacity for adsorption due to their interior tube cavity's unique layout and hydrophobic surface (Akinpelu et al., 2019). Along with conventional adsorbents, graphene oxide, multifunctional nanocomposites, mesoporous molecules, and electric nanofibrous membranes have been employed as effective adsorbents for phenanthrene removal from aqueous solution (Xiong Yang et al., 2019). Nevertheless, nanocomposite materials with a rising water dispersibility might affect the possibility of secondary pollution. Additionally, using standard methods such as filtration, and centrifugation recovering the nanocomposite from the processed aqueous matrix may result in material damage (Zhao et al., 2018). The employment of classic separation technologies in a large-scale actual water purification process may extend the time, and monetary expenditure that is incompatible with the application of sustainable chemistry (Wei et al., 2022). To address these issues, photocatalytic degradation is a technique that is environmentally favourable and produces no secondary pollution, especially when a range of pollutants are destroyed efficiently. Reactive oxygen species have been linked to the degradation of pollutants. Carbon-based compounds like graphene, fullerenes, carbon nanotubes,

and activated carbon have demonstrated promise because of their potential to mix with heterojunction compounds (heterojunction compounds or integrated multi-semiconductor systems provide substantial advantages for increasing the separation of electron-hole pairs and maintaining two distinct reaction sites for reduction and oxidation) to boost photo-efficiency. The development of multifunctional photocatalytic materials has been greatly aided by the use of graphene and its derivatives (Raja et al., 2019, 2020). Zinc oxide (ZnO) is one of the common catalysts with its greater exciton binding energy (60 meV), larger intrinsic electron motility ($300 \text{ cm}^2/\text{V}\cdot\text{s}$), and broad bandgap (3.37 eV). ZnO semiconductors were employed as an excellent catalyst to remove organic contaminants (Sierra-Fernandez et al., 2017). ZnO is a better catalyst than TiO_2 based on several research (Kumar et al., 2014). ZnO semiconductor materials have gained a lot of popularity in recent years because of their wide range of applications, ease of use, high conductivity, and outstanding photocatalytic performance. The bandgap of ZnO materials is quite large, and their nanostructures come in a wide range of configurations. Pollutants are decomposed catalytically with remarkable efficiency. As one of the most common photocatalysts, ZnO is fast becoming a replacement for TiO_2 due to its high sunlight consumption (Kumar et al., 2020; Saravanan et al., 2018). Since ZnO can transport more electrons and holes in response to applied energy, it has greater conductivity. ZnO is a semiconductor that, when combined with other chemicals, ZnO can provide a highly conductive material with useful applications in electronics (Dutta et al., 2021). Kumaresan et al., (2017) found that hydrothermal hydrolysis can produce a wide range of ZnO nanostructures by changing the pH. Hexagonal discs, spindle nanorods, and floral nanorods were introduced at pH values of 7, 9, 11, and 13. The combination of holes and electrons is a key issue that has a negative impact on the

efficiency of ZnO-based photocatalysts, limiting their effectiveness. As a result, multiple tactics were used to inhibit electron-hole recombination and increase ZnO's photocatalytic effectiveness. Fen. Li et al., (2015) investigated that due to its high surface area, mechanical stability, and tunable electrical and optical properties, GO, the functionalized graphene with oxygen-containing chemical groups, has recently received renewed interest. Also, GO is a great option for coordinating with other materials or molecules due to the presence of hydroxyl, epoxy, and carboxyl functional groups on its surface. GO and its composites show significant potential for numerous energy storage and conversion and environmental protection applications due to their increased structural variety and enhanced overall characteristics. These uses include materials that store hydrogen and photocatalysts for splitting water, as well as getting rid of pollutants in the water and cleaning water. One of the effective methods was the addition of GO and metal nanoparticles to boost the photocatalytic efficiency of the material (Al-Rawashdeh et al., 2020). It was also identified that microwave irradiation might be used to make GO-CuO nanocomposites, and the impact of GO on the photocatalytic performance of the CuO catalyst for deterioration of organic pollutants after 60 minutes of ultraviolet irradiation was investigated. The generated GO-CuO nanocomposite was shown to be 4.48 times more efficient than pure CuO. Additionally, it is identified that raising the GO ratio accelerates deterioration (Darvishi et al., 2017). This is primarily owing to the synergetic impact of GO and metal oxides on electron-hole dissociation but also because the occurrence of GO enhanced the probability of adsorption of contaminants on the nanocomposite's surface (Bai et al., 2013; Bhunia & Jana, 2014). Because of the ability of noble metals to promote photoactivity, the use of noble metal hybrids in semiconductor photocatalysts has received considerable interest recently (Rosu et al.,

2017). Hybrid photocatalysts with various GO/ZnO weight ratios were manufactured using a hydrothermal method (Zhang et al., 2014). It was identified that when exposed to organic contamination, GO composite had a more significant photodegradation potential than ZnO under UV irradiation. The GO-ZnO nanoparticles had more efficiency than ZnO itself. ZnO photocatalytic activity could be improved by using GO because of its excellent phenanthrene degradation and charge separation capabilities (Mydeen et al., 2020; Sun et al., 2018). Distinct porous structure, electrochemical characteristics, acidity, and adsorbing capacity make carbonaceous materials a significant asset in the field. Graphene, activated carbon, and carbon nanotubes are among the products that fall under this category of materials. One of the advanced applications of carbon-based composites is the removal of water pollutants by methods like photocatalysis and adsorption. The integration of graphene and ZnO is expected to be suitable for delivering superior photocatalytic efficiency due to the combined graphene structure, which allows charge separation for photocatalysis (Ahmad et al., 2013). Meanwhile, GO has increased interest as it has the same properties as graphene and unique surface structures for the manufacture of GO-containing nanomaterials, in conjunction with the added carboxyl and hydroxyl groups (Li et al., 2012). Few studies predict phenanthrene as a future water pollutant. Typical water treating methods including ozonation and chlorination appear to be unsuccessful in removing and decomposing many hazardous water pollutants (Fu et al., 2018). As a result, some current research studies have focused on the treatment of phenanthrene through photocatalysis as shown in [Figure 1.1](#).

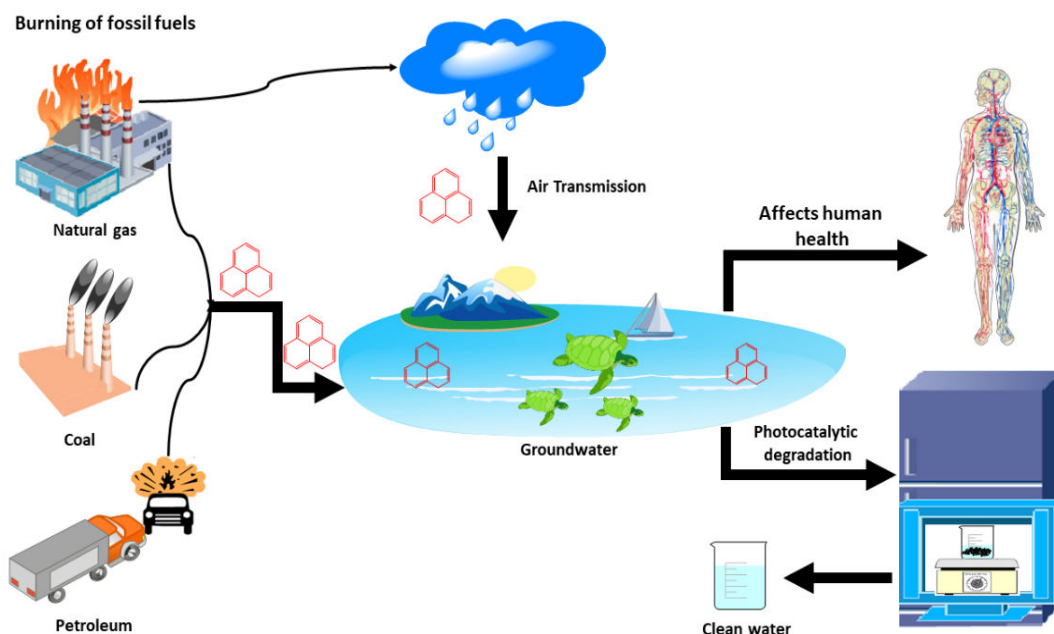


Figure 1.1 Schematic representation of environmental remediation of phenanthrene by photocatalysis.

In this work, a photocatalytic method for removing phenanthrene from contaminated water in the presence of UV-Visible irradiation using GO/ZnO nanoparticles has been explored. Many parameters such as photocatalyst dose, pH, phenanthrene concentration, and reaction kinetics were determined to achieve maximum degradation. Separate studies were also performed in dark conditions and in the presence of UV-Visible irradiation to validate enhanced photocatalytic activity of GO/ZnO through photo-induced electron transfer among metallic ions as well as phenanthrene. By detecting byproducts in UV-Visible light exposed samples, degradation pathways were shown. The nanocomposite has been characterized by Fourier transform infrared, UV-visible diffuse reflectance spectroscopy, X-ray diffraction, Scanning electron microscopy with Energy dispersive X-ray, Brunauer-Emmett-Teller, Transmission electron microscopy, and Raman spectroscopy. As a result, the effectiveness of the photocatalyst was thoroughly studied concerning several factors such as phenanthrene concentration, the dosage of GO/ZnO

nanocomposite, pH, reaction kinetics, and reusability. To aid in the photocatalytic degradation of phenanthrene, the greatest photodegradation efficiency was calculated in comparison to previous research and minor by-products are identified using GC-MS.

1.1.1 Problem statement

Water shortage is a growing concern, with more people being deprived of safe drinking water every day. Industrial effluents contaminate water sources, and other industrial operations are incorporated into water supplies. Among the pollutants identified in the manufacturing sector effluents include phenanthrene. The decomposition of organic pollutants like phenanthrene has been attempted using a rice husk derived nanocomposite. The mineralization of phenanthrene into comparatively innocuous compounds (CO_2 , H_2O) is a function of advanced oxidation processes (AOPs), which are based on the in-situ formation of highly reactive species (HO^\bullet , $\text{O}_2^{\bullet-}$) (Lee & Park, 2013). Chemical oxidation (O_3 , Fenton reagents), photochemical oxidation (UV/ O_3 , UV/ H_2O_2), and heterogeneous photocatalysis (UV/GO-ZnO) are all examples of advanced oxidation processes (AOPs) (Hidalgo et al., 2007; Malato et al., 2007). Photocatalysis stands out because it can produce highly reactive hydroxyl radicals using only visible light and no other chemicals (Lin et al., 2015). For the complete mineralization of phenanthrene and by products, the mild operating conditions of temperature and pressure and the use of chemically stable catalyst (GO/ZnO) are particularly desirable. Photocatalysis has emerged as a promising solution to the growing awareness of the benefits of solar-powered pre- and post-treatment for wastewater.

Previous work reported for the removal of phenanthrene suggests that the wide band gap of ZnO prohibits the successful use of the entire solar spectrum because it only

absorbs the ultraviolet irradiation (4% of the solar light) resulting in weak photocatalytic behaviour (Pal et al., 2015).

Coupling GO derived from rice husk with ZnO has been shown to significantly improve the removal efficiency of photoinduced charge carriers due to creating a heterojunction configuration between them, increasing the catalytic efficiency and photo-stability of the hybrid nanocomposite. However, even though the binding energies of ZnO and GO are comparable, the potential outcomes of the conduction and valence bands of ZnO are somewhat more negative than those of GO (Liou & Wang, 2020). Kamarulzaman et al., (2015) investigated that band gap widening in nanostructured materials occurs via a complex method. The increased downward shift of the VB is primarily responsible for the widened band gap in nanostructured ZnO. Doped compounds (GO) have a narrower band gap in comparison to pristine ZnO, substantially because the CB shifts lower for both nanostructured and micron-sized materials. Therefore, whether the crystallites are nano-or micron-sized and what elements are used in the doping process for narrowing and widening the band gap in substances, the procedure is very complex. Upon irradiation, electrons flow from the CB of ZnO to the CB of GO while holes migrate from the VB of GO to the VB of ZnO, lowering the recombination rate of the pairs. Thus, charge separation efficiently boosts charge carrier lifespan and improves the efficiency of interfacial charge transfer to adsorbed substrates.

It is owing to its exceptional and one-of-a-kind physiochemical features. GO/ZnO, for example, demonstrates extraordinary resistance to photocatalytic degradation, particularly in hostile aquatic environments. In addition, the VB hole has a high oxidation potential for harmful chemicals in the environment. Furthermore, by adding defects in the crystal lattice (altering stoichiometry) and by doping, the

characteristics of GO/ZnO may be significantly altered. Finally, GO/ZnO is substantially reliable than other photosensitive materials, and its reserves are plentiful. So far, all of these considerations place GO/ZnO ahead of different heterogeneous photocatalysts for energy and environmental applications.

Green synthesis and photocatalytic efficacy for eliminating phenanthrene from GO/ZnO nanocomposite are unreported in the literature so far. Because of its widespread dispersion and hazardous potential, this molecule must be tracked and eliminated from the environment. To our knowledge, rice husk derived GO/ZnO nanocomposite has never been tested as a possible photocatalyst under ultraviolet-visible irradiation.

1.1.2 Research questions

1. What was the route taken in the synthesis of GO and GO/ZnO nanocomposites? What did the investigation into GO/ZnO nanocomposites reveal?
2. What are the factors (effect of phenanthrene concentration, effect of GO/ZnO dosage, reaction kinetics, effect of pH, effect of UV-Visible light, and reusability of the photocatalyst) which affects the degradation performance?
3. How well GO/ZnO nanocomposite, photolysis (without a photocatalyst), GO/ZnO without stirring, GO/ZnO in the dark with stirring, and commercial ZnO break down phenanthrene in aqueous solutions under optimal conditions?

1.1.3 Objectives

The main objective of this proposed work is to treat phenanthrene from aqueous solution using GO/ZnO nanocomposite. The studies will be carried out with the following specific objectives:

1. To synthesize the GO and GO/ZnO nanocomposite by using modified Hummer's method and doping method, respectively and to characterize the physicochemical properties of GO/ZnO nanocomposite.
2. To determine the photocatalytic activities (For e.g., effect of phenanthrene concentration, effect of GO/ZnO dosage, effect of pH, and effect of UV-Visible light) for the degradation of phenanthrene from aqueous solutions using GO/ZnO nanocomposite.
3. To compare the effectiveness of GO/ZnO nanocomposite, photolysis (without photocatalyst), GO/ZnO without stirring, GO/ZnO in the dark with stirring, and commercial ZnO in degrading phenanthrene from aqueous solutions under optimal conditions.

1.1.4 Scope and approach

As was previously noted, ZnO has certain remarkable qualities that make it useful in energy and environmental remediation. Unfortunately, it has severe flaws in

(i) rapid recombination of electron and hole pairs and

(ii) only being able to absorb light in the UV spectrum.

ZnO can only absorb light in the UV range since its bandgap is only about 3.3 eV (Rachna et al., 2019b). This portion accounts for only 4% of total incoming solar radiation. Since the visible spectrum accounts for roughly 42% of solar radiation, it is crucial to increase ZnO's light absorption in this region for solar radiation applications. ZnO's rapid e-h pair recombination is also counterproductive because it causes the absorbed energy to be released as heat or radiated without being put to any practical chemical use. These two natural properties of ZnO contribute a lot to its low quantum efficiency and make it hard to use in many different ways. There are several ways to reduce their impact significantly. The problems of charge carrier dynamics

and light absorption are tackled in this thesis by designing and preparing ZnO-based nanocomposite systems. Understanding the underlying processes of the improved photocatalytic activity has received particular focus. The prepared photocatalysts are as follows:

This model system of ZnO/Carbon nanocomposites has been developed to investigate the effect of electrically conductive carbon films, such as graphite and graphene, on the photocatalytic efficiency of ZnO nanostructures. The interfacial interactions of carbon underneath ZnO and the dynamics of charge carriers have received particular attention. Much research has been done on how the way GO derived from rice husk is made affects how well ZnO works as a photocatalyst.

By combining the GO solution derived from rice husk and ZnO solution in a 1:2 mol ratio, a GO/ZnO photocatalyst was created. The ZnO solution was then mixed directly with the GO solution with continuous stirring to create a GO/ZnO nanocomposite. To find the best photocatalyst, Fourier transform infrared (FTIR) spectroscopy, energy dispersive x-ray (EDX), X-ray Diffraction (XRD), Scanning Electron Microscopy (SEM), Ultraviolet-Visible Diffuse Reflectance Spectroscopy (UV-Vis DRS), Transmission Electron Microscopy (TEM), Brunauer-Emmett-Teller (BET), Raman spectroscopy were carried out. To understand the high photocatalytic activity in the optimised sample, information on the surface morphology, crystal structure, photocatalytic activity, and optical band gap was acquired.

After selecting the most effective photocatalyst, several factors were studied to determine how they affected photocatalytic activity in phenanthrene degradation. These factors included phenanthrene concentration, GO/ZnO dosage, pH, reaction kinetics, UV-Visible light, and the photocatalytic degradation routes of phenanthrene utilizing the nanocomposite.

1.1.5 Significance

Photocatalysis technologies aided by nanocomposites are gaining popularity with diverse applications in the environmental sphere. The capacity to harness the high potential of photoactive nanoparticles and get accessibility to their capabilities is based upon the ability to incorporate them into photoreactors and distribute them efficiently on broad surfaces. To develop processable nanocomposite materials, it is critical to include nanoparticles in appropriate host matrices before incorporating them into functional structures and, eventually, devices. The synthesis of photocatalytic nanocomposite materials and their use for pollutant degradation are thoroughly discussed. We concentrate on contemporary synthetic techniques for synthesizing UV and visible light active photocatalysts, surface functionalization after synthesis, and inclusion in appropriate host matrices for nanocomposite creation.

1.1.6 Thesis organization

The following is the format of this thesis report:

Chapter 1 provides a brief overview of the research background, including water pollution caused by various organic pollutants such as polycyclic aromatic hydrocarbons (phenanthrene), various methods to treat polluted water, including photocatalysis using various nanocomposites, including GO/ZnO, basic properties and applications of GO/ZnO, development and advantages of using GO/ZnO nanocomposite for photocatalysis, problem statement, research questions, objectives, and scope and approach, and significance, as well as thesis organization.

Chapter 2 presents a complete overview of the literature on the photocatalytic degradation of phenanthrene and the mechanism and degradation pathways of phenanthrene. The first part of this chapter discusses the photocatalytic degradation

of phenanthrene by describing the process in detail. The second part compares different types of the commonly used photo-catalysts, focusing on GO/ZnO nanocomposite. The third part analyses the mechanism of photocatalytic degradation through different catalysts and the degradation products formed by different catalysts, and the pathways involved in the degradation of phenanthrene. The last part of this chapter covers the summary of the literature for finding the research gaps and the solutions for filling this gap.

Chapter 3 describes the detailed experimental procedures in this project. The first part discussed the flow chart of the experiment for the photo-degradation of phenanthrene under UV-Visible light. The second part gives all the materials and chemicals used, and the third part describes the steps for preparing the GO/ZnO nanocomposite. The characterization techniques and equipment used are mentioned in the fourth part. The last section describes the experimental setup, methodologies, and theoretical support used to assess the photocatalytic efficiency of the GO/ZnO nanocomposite.

Chapter 4 presents the findings of several characterization methods and the photocatalytic activities of the GO/ZnO nanocomposite. This section also includes an in-depth examination and comparison of the outcomes.

Chapter 5 concludes the work done on this project and gives recommendations for future work. Finally, the bibliography part provides the references used in this thesis report.

CHAPTER 2

LITERATURE REVIEW

2.1 Photocatalytic degradation of phenanthrene

PAHs are a class of persistent organic pollutants (POPs) that result from incomplete combustion of fossil fuels, industrial production, oil spills, and natural sources (Yu et al., 2018). Chronic exposure to PAHs, even at low concentrations, can have long-term effects on humans, including infertility, cancer, and neurotoxicity (Qiao et al., 2014a). Because of their high hydrophobicity, PAHs' toxicity can be increased by their bioaccumulation in human tissue (Yu et al., 2018). Because of their extreme toxicity, the US Environmental Protection Agency (EPA) has designated 16 PAHs as priority pollutants (Fu et al., 2018). The content of PAHs in numerous rivers investigated ranges from 0.16–1.20 $\mu\text{g/L}$ (dissolved phase) and 1.56–79.38 $\mu\text{g/g}$ (particulate phase) (Qiao et al., 2014b). As a result, removing PAHs from the water phase is still a popular issue in environmental research. Due to its exceptionally stable three-ring structure, phenanthrene is one of the most commonly identified PAHs in aquatic settings with quite high concentrations, and it is durable and difficult to decompose. Except in extremely industrially contaminated rivers, individual PAH concentrations in surface and coastal waters are typically 50 ng/l (World Health Organization, 2003). Zeng's team conducted a PAH survey in 42 freshwaters around China, and phenanthrene was shown to be one of the most prevalent parent PAHs (Yao et al., 2017). In addition, a countrywide investigation of PAHs in drinking water indicated that phenanthrene is the most prevalent individual PAH in tap water, accounting for 33% of the total 16 USEPA-listed priority PAHs; also, 3-ring PAHs (e.g., phenanthrene) are much harder to remove in the drinking water treatment process than

other PAHs (Ying Zhang et al., 2019). Adsorption, biodegradation, chemical oxidation, and other techniques have been used to remove PAHs and other organic pollutants from water. Yu et al. (2018), for example, used a novel citric acid chelated-Fe(II) activated persulfate/percarbonate system to remove phenanthrene in aqueous phase; the chelated complex increased Fe(II) solubility, and the system produced a large amount of $\cdot\text{SO}_4^-$ and $\cdot\text{OH}$, resulting in high phenanthrene removal efficiency at optimal persulfate-percarbonate ratio. However, the intrinsic restrictions of either low efficiency or excessive energy/chemical consumption preclude its use (Kou et al., 2009). Photocatalytic degradation of pollutants using solar light is a green and sustainable method that has received a lot of attention recently (Liu et al., 2017). The primary method for a competent semiconductor photocatalyst is that the e^-/h^+ redox potential charging carriers must fall inside the catalyst bandgap. Previous work reported for the removal of phenanthrene indicated that the wide bandgap of TiO_2 , NiO , In_2O_3 , and $\alpha\text{-Fe}_2\text{O}_3$ prohibits the successful use of the whole solar system since it only captured the UV rays (4% of the sunlight). To improve the light absorption range and to reduce the recombination rates for e^-h^+ pairs of ZnO , TiO_2 , NiO , In_2O_3 , $\alpha\text{-Fe}_2\text{O}_3$, various protocols were adopted. Recent studies show that in addition to this combination of metals, the amalgamation of ZnO , TiO_2 , NiO , In_2O_3 , $\alpha\text{-Fe}_2\text{O}_3$ with GO also demonstrated its propitiousness as an effective photocatalyst.

About half the world's population relies on rice as a staple meal (Hossain et al., 2021). In addition to China and India, Indonesia is also a significant producer. As a by-product of the rice-growing process, rice husk is a common source of garbage in many nations (Siddika et al., 2021). Rice husks are the hard protective coat that protects the paddy grain from damage and are removed from the rice seed during milling (Hossain et al., 2021). They are lignocellulosic materials, and it was calculated that milling five

tonnes of rice paddy results in one tonne of rice husk, for a total yearly production of around 120 million tonnes of rice husk (Chandrasekhar et al., 2003). Massive amounts of rice husk are produced, making their repurposing as a biofuel source and an industrial heat source essential (Abbas & Ansumali, 2010). Using rice husk as a fuel source in industries, rather than coal, would help reduce carbon emissions from coal burning, which would be in line with a directive on waste management from the European Union (European Union, 2009). RHA, which roughly constitutes 20–25% of the weight of rice husk, is a by-product created when rice husk is burned as fuel in the boiler (Jittin et al., 2020). Rice husk has good anti-corrosion capabilities against steel, aluminium, and copper and is very resistant to the action of hazardous fungi. Since rice husk is abundant and chemically stable, it may serve as a precursor to producing high-quality graphene, which can be further oxidized to GO from agricultural waste, as suggested by the provided analysis (Ismail et al., 2019).

GO is a zero bandgap semiconductor that can absorb more visible light, thus improving the photocatalytic efficiency, and has a work function of -4.42 eV (Liu et al., 2016). The findings suggest that compared to pristine ZnO, TiO₂, NiO, In₂O₃, α -Fe₂O₃, the photoluminescence peak of GO with these composites is much lower, so GO serves as a path of electron migration while reducing the recombination of photogenerated e^-h^+ pairs in the hybrids in TiO₂, ZnO, NiO, In₂O₃, and α -Fe₂O₃. GO and ZnO formed a heterojunction in the photodegradation mechanism of phenanthrene with GO/ZnO nanocomposite, which assisted the separation of photogenerated carriers. The band gaps of ZnO and GO have been 3.23 eV and 0.02 eV, respectively. GO, and ZnO was excited to yield electrons and the holes at conduction band (CB) as well as the valence band (VB), respectively, during sunlight irradiation, as described in [Figure 2.1](#). Because the ZnO band positions were underneath the CB and VB of

GO. The photoexcited electrons migrated from GO to ZnO, while the holes transferred from ZnO to GO. Whereas the molecules of oxygen in the solution of phenanthrene reacted with the electrons, it produces superoxide radical ($\cdot\text{O}_2^-$), and the holes react with H_2O to generate hydroxyl radical ($\cdot\text{OH}$).

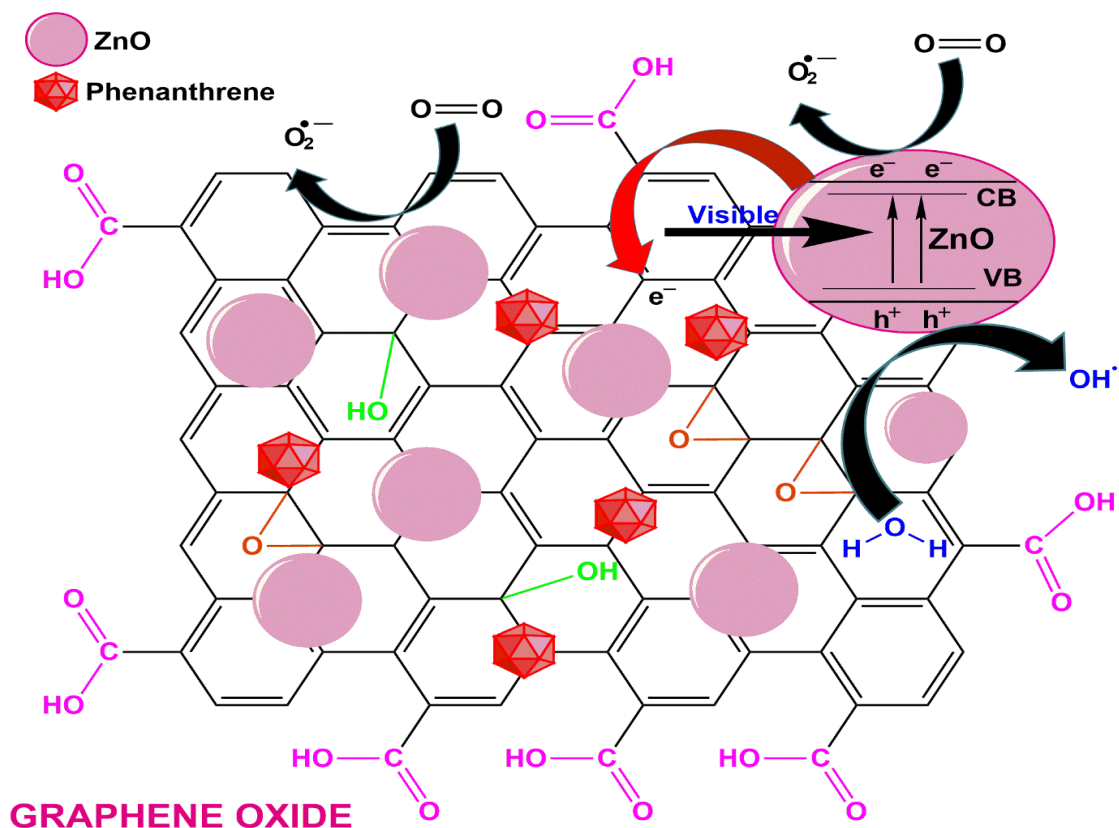


Figure 2.1 The implemented degradation of phenanthrene by photocatalysis intervened by GO/ZnO nanocomposite.

On the other hand, the phenanthrene has been directly oxidized through the holes at the VB of GO. The ($\cdot\text{OH}$ and $\cdot\text{O}_2^-$) potent oxidizing radicals immediately oxidized the molecule of phenanthrene. In the presence of sunlight, Shanmugasundaram et al., (2018) developed the following probable degradation process of phenanthrene with GO/ZnO. The incident photon generates the pairs of electron-hole (e^-h^+) on the photocatalyst's surface changing poisonous organic pollutants into nontoxic by-products through the kinetics process of reduction and oxidization. The overall

findings of the studies indicate that the final products from the reaction of photocatalysis are generally found as CO₂ and H₂O.

2.2 Types of photocatalysts for the degradation of phenanthrene

2.2.1 Titanium dioxide-based photocatalysts

Wen et al., (2002) studied that the degradation processes of phenanthrene through photocatalysis at TiO₂/water interfaces. Phenanthrene with low aqueous solubility could be quickly degraded in aqueous dispersion under UV irradiation after preadsorbing to TiO₂. The diffusion pH, the contact area, and the composition of ph/TiO₂ seemed to have no impact on the photodegradation intensity of TiO₂ catalysed phenanthrene. Many transitional compounds provided hydroxylation, ring-open reaction, and ketolysis with higher absorption along with the ease of decomposition. Phenanthrene could be photo-oxidized easily and eventually oxidized to CO₂ within prevailing circumstances.

P123 was used as a template for a one-pot process to synthesize a thiol-functionalized nano photocatalyst MPTES/TiO₂. The complete anatase crystalline of thiol-functionalized TiO₂ confirmed by X-ray diffraction and N₂ adsorption-desorption isotherm shows the highest surface area and mesoporic configuration of these materials. To test the photocatalytic behaviour of these materials, the degradation of phenanthrene through photocatalysis under solar light (wavelength > 420 nm), a potential mechanism was suggested based on the experimental results of the GC–Mass analysis (Liu et al., 2009).

In a surfactant solution containing TiO₂ particles, the heterogeneous photocatalytic degradation of phenanthrene was studied. The degradation ratio of phenanthrene increased from 0.1 gram/litre to 0.5 gram/litre with the rise of TiO₂. The surfactant

micelles can have a non-aqueous 'cage' and lead to a higher rate of degradation of the phenanthrene than the aqueous solution. On the other hand, greater than 2 gram/litre of Triton X-100 reduced the phenanthrene deterioration ratio. The phenanthrene deterioration ratio in the basic medium appeared greater than that in the acidic solution since the greater pH estimation might also create hydroxyl ions in higher concentration to combine with the holes to generate hydroxyl radicals. When O₂ and H₂O₂ were applied to the suspension, it improved the photodegradation process rate, which created a synergistic effect (Yanlin Zhang et al., 2011).

It was suggested for the first time that dimethyl carbonate (DMC) can possibly an environmental friendly solvent for photocatalytic synthesis. The paradigm of the green synthetic method, beginning with PAHs, was described as a part of the photocatalytic oxidation of phenanthrene in dimethyl carbonate with anatase TiO₂ as a photocatalyst (Bellardita et al., 2014). To prepare organic-inorganic co-functional TiO₂ nanomaterial, Zhou et al (2015) adopted an easy one-pot synthesis route. For the photodegradation of phenanthrene, the photocatalytic reactivity of such resulting compounds was assessed under visible illuminations (wavelength > 420 nm).

The link between the degradability of PAHs by photocatalysis in water over Pt/TiO₂-SiO₂ and their molecular structure was also studied. Fluorene, Naphthalene phenanthrene, pyrene, benzo[a]pyrene (BaP), and dibenzo[a]anthracene (DahA) was studied experimentally under UV radiation in Pt/TiO₂-SiO₂. The findings showed that the deterioration of high molecular weight polyaromatics, BaP, pyrene, and DahA was significantly substantially increased in the existence of Pt/TiO₂-SiO₂. In contrast, the decomposition efficacy of low molecular weight polynuclear aromatic hydrocarbons, naphthalene, fluorine and phenanthrene has been hindered under the same experimental parameters (Luo et al., 2015).

A new form of Co-deposited titanate nanotubes (Co-TNTs-600), using Titanium oxide (P25) as prerequisite through a bi-step progression (starting with hydrothermal process at 150 °C followed by calcination process at 600 °C) was employed for excellent photocatalytic oxidation of phenanthrene. Co-TNTs-600 demonstrated immense photocatalytic activity for the deterioration of phenanthrene in sunlight irradiation, with a 98.6% extraction rate of approximately 1 gram/litre dose in 12 hours. The first kinetic model was capable of interpreting the dynamic information properly. The studies show that the possible rate constant was 0.39 h⁻¹, which is 23-fold that of the titanate nanotubes (TNTs) and ten times that of the P25. The collective outcome of calcination/crystallization and Co-deposition culminated in the drastic synergistic effect of Co-TNTs-600. As a result of improved catalytic activity of the Co-TNTs-600, photocatalytic process for phenanthrene appeared comparable to that for certain photocatalysts. 9,10-phenanthrenedione and (1,1-biphenyl)-2,2-dicarboxaldehyde were key intermediate products that were predicted to have been completely mineralized (Zhao et al., 2016). Enhanced adsorbability and photocatalytic operation of TiO₂-graphene composite (P25-GR) were used to remove phenanthrene from amorphous regions. P25-GR photocatalysts were synthesized with various GR addition ratios by hydrothermal process. The P25-2.5% GR demonstrated dominance in elimination of phenanthrene due to its selective adsorption capability and enhanced transport of charges. The composite showed improved photocatalytic efficiency at tremendous phenanthrene concentrations (2.0-4.0 µg/mL) and in a basic medium. Moreover, the conditional declination routes of phenanthrene were correspondingly seen based on the recognition of intermediates (Bai et al., 2017).

It was studied that the consequences of water quality framework and statistical simulation through the degradation of phenanthrene through photocatalysis by

graphite oxide-TiO₂-Sr(OH)₂/SrCO₃ nanocomposite by direct solar radiation. It was found that graphite oxide-TiO₂-Sr(OH)₂/SrCO₃ was prepared and showed off good photocatalytic exertion under atmospheric conditions for the degradation of phenanthrene and high stability underneath a variety of water environments which may be saltwater and with oil dispersing agents. The Photocatalytic progress was due to the speciation of TiO₂ and Sr(OH)₂/SrCO₃ couplings and delocalization of GO sheet electrons. The most critical aspect of the photocatalytic process was the oxidative radicals $\bullet\text{O}_2^-$ and $\bullet\text{OH}$, and thus the dominant degradation pathway was their attack at positions 9 and/or 10 of phenanthrene. In sum, graphite oxide-TiO₂-Sr(OH)₂/SrCO₃ could serve as an extremely efficient and comprehensive photocatalyst for power-efficient degradation of PAHs by photocatalysis in clogged drainage matrices and the multiplicative model was a valuable model for estimating photocatalytic efficiency under different aquatic ecosystems (Fu et al., 2018). It was studied that the efficiency of the home-grown photocatalytic membrane reactor to address the phenanthrene pollution in water medium resulting in the evaluation of slurry photocatalytic membrane reactor (PMR). The research further revealed that during the photocatalytic degradation the total carbon removal efficiency throughout the experiments was found to be 97% while the elimination efficiency was found to be 79 %. Another study to get the information of operability and reusability of PMR shows that TiO₂ can be reused competently with lower permeate fluxes. The major intermediates listed in this report consisted primarily of quinones, ketones and alcohols (Rani & Karthikeyan, 2018).

Titanium dioxide is the lead photocatalyst in all semiconductors with high catalytic effects and is stable for incident photon or chemical decomposition. Phenanthrenes, the tricyclic polyaromatic hydrocarbons, in the water and stream sediments with a

novel heterogeneous TiO₂-based nanocomposite have been analysed, and it was found that the production of simple, economical, green, and thoroughly competent progress for the arrangement of an excellently dynamic TiO₂ assimilated zinc hexacyanoferrate (ZnHCF) nanocomposite was effectively carried out. Shifts obtained in powdered X-ray diffraction, Fourier transform infrared, and the morphological variations have confirmed that the parent materials were assembled into the nanocomposite. Photoluminescence and total organic carbon results determined a principal association of H₂O or O₂ with charge carriers to generate OH % that decreased and ultimately mineralized phenanthrene under sunlight. The nanocatalyst was reusable up to 10 cycles with the extensive lattices of ZnHCF utilised as Zn²⁺ stores around by titanium dioxide, generating synergistic impact as fundamental decomposition mechanism along with charge carriers' reactions. These findings composed the amalgamated green nanocatalyst appropriate for industrial use (Rachna et al., 2019a).

Mutualistic adsorption of Cu (II) and photocatalytic deterioration of phenanthrene by a jaboticaba-like nanocomposite, titanate nanotubes supported TiO₂ (TiO₂/TiNTs) analyzed experimentally as well as theoretically, and the investigation alleged the use of TiO₂/TiNTs to eliminate the organic toxins and the heavy metals cations from water using hybrid adsorption-photocatalysis technique. Having a considerable number of -OH/Na groups, TiO₂/TiNTs offers ample adsorption sites for heavy metal cations, whereas the anatase phase shows elevated photo-catalytic activity. In one of the reports, Cu (II) adsorption on TiO₂/TiNTs reached the equilibrium in 20 minutes with an adsorption capacity of 115.0 mg/g. The photocatalytic study of phenanthrene using TiO₂/TiNTs degraded up to 93 % in 4 hours, the reaction rate suggest that the first order rate constant (K_{obs}) was almost 10 times more than that of pure TiNTs, which suggest more balanced photocatalytic activity of TiO₂/TiNTs after anatase

loading. Results of this analysis showed the immense potential for the separation of heavy metals and organic matter from wastewater by TiO₂/TiNTs nanocomposite (Cheng et al., 2019).

A specific type of WO₃@TiO₂-SiO₂ nanocomposite photocatalyst was already synthesized through simple sol-gel and calcination. Prepared photocatalyst demonstrated more than seven times greater photocatalytic behaviour for phenanthrene oxidation in visible light than commercial TiO₂ (P25). During phenanthrene degradation, 9,10-phenanthrenediol, 9-phenanthrenol, and 9,10-phenanthrenedione were formed as the dominant transitional compounds and based on analysed transitional compounds, and density functional theory (DFT) measurements, the degradation pathway of phenanthrene was suggested (Cai et al., 2019).

Therefore, the investigation was conducted that concentrated on the photocatalysis based degradation of phenanthrene using titanium dioxide-based photocatalysts and its various parameters are listed in [Table 2.1](#).

Table 2.1 List of titanium dioxide-based photocatalysts and its various parameters for the degradation of phenanthrene.

S. N.	Photocatalyst	Experimental conditions	Detector/ column	Light intensity	Wavelength λ (nm)/ Light power	Reaction kinetics	Efficiency (%)	References
Titanium dioxide-based photocatalysts								
1.	Aqueous TiO ₂ suspensions	pH: 2 - 10; temp.: NA; dose: 50 mg; time: 90 min; conc.: 5.6×10^{-5} mol/g	GC-MS, Trio-2000/ BPX 70 column (30m \times 0.25 mm)	30 mW/m ²	>320/100 W	-	Over 90	(Wen et al., 2002)
2.	Titania immobilized on a quartz tube	pH: NA; temp.: 325 °C; dose: 2.128 g; time: 3 hr; conc.: 9.653×10^{-6} mol	Cylindrical glass reactor (38.2 cm long & 0.6 cm i.d) fabricated & quartz rod (38 cm long & 0.3 cm i.d)/ column Phenomene	8.1 mW/cm ²	>290/-	Linear isotherm	35 to 67	(Lin & Valsaraj, 2003)